Fabrication of Heterostructured Fe_2TiO_5-TiO_2 Nanocages with Enhanced Photoelectrochemical Performance for Solar Energy Conversion

*Peng Zhang, Xue Feng Lu, Deyan Luan, and Xiong Wen (David) Lou**

[*] Dr. P. Zhang, Dr. X. F. Lu, Dr. D. Y. Luan, Prof. X. W. Lou

School of Chemical and Biomedical Engineering, Nanyang Technological University, 62 Nanyang Drive, Singapore, 637459, (Singapore)

Email: xwlou@ntu.edu.sg; davidlou88@gmail.com

Webpage: http://www.ntu.edu.sg/home/xwlou/

Abstract

Photocatalysts with well-designed compositions and structures are desirable for achieving highly efficient solar-to-chemical energy conversion. Heterostructured semiconductor photocatalysts with advanced hollow structures possess beneficial features for promoting the activity towards photocatalytic reactions. Here we develop a facile synthetic strategy for the fabrication of Fe_2TiO_5-TiO_2 nanocages (NCs) as anode materials in photoelectrochemical (PEC) water splitting cells. A hydrothermal reaction is performed to transform MIL-125(Ti) nanodisks (NDs) to Ti-Fe-O NCs, which are further converted to Fe_2TiO_5-TiO_2 NCs through a post annealing process. Owing to the compositional and structural advantages, the heterostructured Fe_2TiO_5-TiO_2 NCs show enhanced performance for PEC water oxidation compared with TiO_2 NDs, Fe_2TiO_5 nanoparticles (NPs) and Fe_2TiO_5-TiO_2 NPs.

Keywords: metal-organic frameworks; heterostructures; nanocages; Fe_2TiO_5, TiO_2.

The fast-increasing energy demand and environmental issues caused by the consumption of traditional fossil fuels urge the development of renewable energy sources.[1,2] Among different types of clean energy, the solar energy is considered to be promising.[3] Solar energy possesses the advantages of inexhaustibility, universality, high capacity and environmental benignancy, while the decentralized and intermittent nature of insolation is still a great challenge for its practical applications.[4,5] An effective solution for this problem is to convert solar energy to the forms that are flexible for end consumptions.[6,7] For instance, photoelectrochemical (PEC) water splitting for the production of hydrogen and oxygen could convert solar energy into chemical bonds.[8] These products of the photocatalytic processes can be used in many applications, such as industrial reactions, fuel cells and aviation.[9] Since the efficiency of a PEC water splitting cell is mainly affected by the photocatalytic activity of the electrode materials, it is essential to design photocatalysts with high performance, low cost and long-term stability.[10]

TiO_2 has been widely studied as one of the most important photocatalysts for several decades due to the high activity and stability.[11] With the relatively large band gap of 3.0-3.2 eV, most TiO_2 photocatalysts could only utilize the ultraviolet (UV) part of the solar spectrum.[12] Since the energy of UV light takes up a relatively low fraction of the whole solar spectrum, the theoretical efficiency of TiO_2 for PEC water splitting is not sufficient for practical solar-to-chemical energy conversion systems.[13,14] To address this issue, Fe_2TiO_5 has been selected to build heterostructures with TiO_2.[15] The narrow band gap of Fe_2TiO_5, which is about 2.2 eV, ensures the absorption and utilization of visible (Vis) light. At the same time, Fe_2TiO_5 has suitable band edge positions and appropriate atomic structures to realize both the water oxidation reaction and the fast charge separation/transfer within Fe_2TiO_5-TiO_2 heterostructures. Therefore, high-efficiency PEC water splitting cells would be fabricated with heterostructured Fe_2TiO_5-TiO_2 photoanodes.

Another important strategy to enhance the performance of semiconductor photocatalysts is through the design of advanced structures.[16] Among various material architectures, hollow structures exhibit distinct advantages for solar-to-chemical energy conversion.[17] The large surface area of hollow-structured photocatalysts would provide a large number of active sites. The thin-shelled topology could shorten the distance for the transfer of charges, thus accelerate the separation of photogenerated electrons and holes. Moreover, the light scattering effect in hollow structures would promote the light absorption ability of the material. Most recently, synthetic approaches based on metal-organic frameworks (MOFs) have been proved effective for the fabrication of well-defined hollow structures.[18] The unique physical and chemical properties of MOF materials would provide great flexibility for the design of hollow-structured photocatalysts with desired features.[19]

Herein, we have developed a facile synthetic strategy to fabricate Fe_2TiO_5-TiO_2 nanocages (NCs) for PEC water oxidation (**Figure 1**a). Specifically, MIL-125(Ti) (MIL: Matérial Institut Lavoisier) nanodisks (NDs) are first synthesized by a conventional solvothermal approach (see the Supporting Information for the experimental details).[20,21] Field-emission scanning electron microscopy (FESEM) and transmission electron microscopy (TEM) images of MIL-125(Ti) show that the sample is uniform with a disk-like morphology (Figure 1b-d). The sharp diffraction peaks at 2θ of 6.9°, 9.8°, 11.8° and 19.7° in the X-ray diffraction (XRD) pattern confirm the formation of MIL-125(Ti) (Supporting Information, Figure S1a).[22] Energy-dispersive X-ray (EDX) spectrum of the sample reveals the existence of Ti, C and O elements, which also verifies the successful synthesis of the MIL-125(Ti) NDs (Supporting Information, Figure S1b).

Subsequently, the as-prepared MIL-125(Ti) NDs are converted to Ti-Fe-O NCs through a hydrothermal reaction. As indicated by the XRD pattern, the obtained sample is amorphous (Supporting Information, Figure S2a). EDX spectrum indicates that the Ti/Fe atomic ratio is about 2:1

(Supporting Information, Figure S2b). FESEM images of the sample show that the disk-like morphology is preserved, while the surface becomes rough (**Figure 2**a,b). Close observation of one broken particle indicates the generation of some void space inside, suggesting the formation of a hollow structure (Figure 2c). TEM image at a relatively low magnification further confirms the formation of Ti-Fe-O NCs (Figure 2d). Moreover, the hollow structure of Ti-Fe-O NCs is well-defined according to the TEM observations from the side and top (Figure 2e,f). TEM image at a high magnification indicates that the Ti-Fe-O NCs are mesoporous and constructed by nano-sized particles (Figure 2g). As shown in the high-angle annular dark-field scanning transmission electron microscopy (HAADF-STEM) and elemental mapping images, Fe, Ti and O are distributed uniformly in the Ti-Fe-O NC (Figure 2h,i). These results indicate that the MIL-125(Ti) NDs are successfully converted to Ti-Fe-O NCs through the hydrothermal reaction.

The Ti-Fe-O NCs are then deposited on a piece of fluorine-doped tin oxide (FTO) glass through the electrophoretic deposition method in a constant voltage mode.[23] The obtained electrode is further annealed at a high temperature of 800 ºC for 10 min to fabricate the Fe_2TiO_5-TiO_2 NC photoanode. Top-view and side-view FESEM images of the photoanode show that a film consisting of the Fe_2TiO_5-TiO_2 NCs is formed on the surface of the FTO glass (**Figure 3**a,b). The thickness of the film is about 7 μm. XRD pattern of the sample shows diffraction peaks at 2θ of 18.2º, 25.5º and 32.5º, confirming the formation of Fe_2TiO_5 (Supporting Information, Figure S3a).[24] Simultaneously, the diffraction peaks at 2θ of 27.3º and 36.2º could be assigned to rutile TiO_2. The XRD pattern indicates the formation of Fe_2TiO_5-TiO_2 heterostructures.[25,26] According to the EDX spectrum (Supporting Information, Figure S3b), the Ti/Fe atomic ratio of Fe_2TiO_5-TiO_2 NCs is 1.9:1, which is similar to that of the Ti-Fe-O NCs. This result indicates that the estimated molar ratio of Fe_2TiO_5/TiO_2 is about 1:2.8. No apparent morphological change is found after the annealing process as shown in the FESEM images (Figure

3c,d). At the same time, the hollow structure of the Ti-Fe-O NCs is inherited (Figure 3e). TEM images indicate that the Fe_2TiO_5-TiO_2 NCs possess well-defined hollow structures with thin shells (Figure 3f-h). The lattice spacings of 0.490 nm and 0.324 nm in the high-resolution TEM (HRTEM) image correspond to the (200) planes of Fe_2TiO_5 nanocrystals and the (110) planes of TiO_2 nanocrystals, respectively (Figure 3i). The diffraction rings observed in the selected area electron diffraction (SAED) pattern imply the polycrystalline nature of the sample, which can be assigned to the (020), (230) and (240) planes of Fe_2TiO_5 as well as the (110) and (101) planes of TiO_2 (Figure 3j). As shown in the HAADF-STEM and elemental mapping images of a Fe_2TiO_5-TiO_2 NC, Fe, Ti and O elements are distributed uniformly (Figure 3k,l). Therefore, heterostructured Fe_2TiO_5-TiO_2 NCs are obtained through the annealing of Ti-Fe-O NCs.

To reveal the compositional and structural advantages of the heterostructured Fe_2TiO_5-TiO_2 NCs for PEC water oxidation, photoanodes constructed with TiO_2 NDs, Fe_2TiO_5 nanoparticles (NPs), and Fe_2TiO_5-TiO_2 NPs are fabricated as control samples (Supporting Information, Figure S4-S9). The PEC performance is evaluated by using a three-electrode cell in an electrolyte containing 1.0 M NaOH. Pt and Ag/AgCl electrodes are used as the counter and reference electrodes, respectively. The low dark current densities indicate that the photocatalysts are almost inactive without light irradiation (Supporting Information, Figure S10). Photocurrent density versus bias (*J*-*V*) curves are collected under simulated air mass 1.5 global (AM 1.5G) irradiation with an intensity of 100 mW cm^{-2}. The TiO_2 NDs exhibit negligible photocurrent density (**Figure 4**a). This phenomenon may be ascribed to the narrow light absorption range of TiO_2 due to the relatively large band gap (Supporting Information, Figure S11). Fe_2TiO_5 NPs, which have promoted light absorption ability, show higher photocurrent density than the TiO_2 NDs. Compared with both TiO_2 NDs and Fe_2TiO_5 NPs, the heterostructured Fe_2TiO_5-TiO_2 NPs show enhanced performance. This result indicates that the heterojunction between Fe_2TiO_5

and TiO_2 could promote the photocatalytic activity. At the same time, the photocurrent density of Fe_2TiO_5-TiO_2 NCs is much higher than that of the Fe_2TiO_5-TiO_2 NPs, revealing the superiority of the well-defined hollow structure. The light scattering effect and formation of heterostructures in the Fe_2TiO_5-TiO_2 NCs would lead to promoted light absorption capability and charge separation efficiency, which could result in the accumulation of photogenerated holes on the Fe_2TiO_5 component for the enhanced water oxidation activity (Supporting Information, Figure S12). The applied bias photon-to-current efficiencies (ABPEs) of different samples show a similar trend as that of the photocurrent densities (Supporting Information, Figure S13). Fe_2TiO_5-TiO_2 NCs exhibit the highest ABPEs compared with the control samples. Incident photon-to-current conversion efficiencies (IPCEs) are measured under monochromic irradiations (Figure 4b). TiO_2 NDs only show IPCEs at the UV-light range, while Fe_2TiO_5 NPs are active under both UV-light and Vis-light, which is in accordance with the light absorption abilities of the materials. The IPCEs of Fe_2TiO_5-TiO_2 NPs are enhanced compared with the single-phase samples. The Fe_2TiO_5-TiO_2 NCs exhibit the highest IPCEs, which reach about 7.3% at 350 nm. Results of electrochemical impedance spectroscopy (EIS) characterizations further reveal that the Fe_2TiO_5-TiO_2 NCs possess the lowest charge transfer resistance for the enhanced PEC performance (Supporting Information, Figure S14). As indicated by the photocurrent density versus time (*J*-t) curve, Fe_2TiO_5-TiO_2 NCs show good stability for PEC water oxidation with slight deactivation after 12 h (Figure 4c). The hollow structure of the Fe_2TiO_5-TiO_2 NCs is maintained after the long-term operation (Supporting Information, Figure S15). The PEC performance of the Fe_2TiO_5-TiO_2 NCs compares favorably to those of some representative Fe_2TiO_5-TiO_2 heterojunction photocatalysts reported for PEC water oxidation (Supporting Information, Table S1).[27-29] However, further improvement is still needed to surpass the high activity of arrayed electrode materials,[15] which would be achieved by enhancing the charge transport between the photocatalyst and substrate.

In summary, novel heterostructured Fe_2TiO_5-TiO_2 nanocages (NCs) have been fabricated through a facile synthetic approach. Uniform MIL-125(Ti) nanodisks are first synthesized as the precursors, which are converted to Ti-Fe-O NCs through a hydrothermal reaction. A subsequent annealing process at high temperature leads to the formation of Fe_2TiO_5-TiO_2 NCs. The enhanced photoelectrochemical performance and stability of the Fe_2TiO_5-TiO_2 NCs indicate that heterojunctions and well-defined hollow structures are essential for promoting the activity of semiconductor photocatalysts towards solar water splitting. The developed synthetic strategy may inspire further capability on constructing hollow heterostructured photocatalysts for efficient solar energy utilization.

Acknowledgements

X.W.L. acknowledges the funding support from the Ministry of Education of Singapore through the AcRF Tier-2 grant (MOE2017-T2-2-003; M4020386), and the National Research Foundation (NRF) of Singapore via the NRF Investigatorship (NRF-NRFI2016-04).

References

[1] K. K. Sakimoto, N. Kornienko, P. Yang, *Acc. Chem. Res.* **2017**, *50*, 476.

[2] P. Zhang, B. Y. Guan, L. Yu, X. W. Lou, *Chem* **2018**, *4*, 162.

[3] C. Ding, J. Shi, Z. Wang, C. Li, *ACS Catal.* **2017**, *7*, 675.

[4] P. Zhang, T. Wang, X. Chang, J. Gong, *Acc. Chem. Res.* **2016**, *49*, 911.

[5] N. S. Lewis, *Science* **2016**, *351*, aad1920.

[6] C. Jiang, S. J. A. Moniz, A. Wang, T. Zhang, J. Tang, *Chem. Soc. Rev.* **2017**, *46*, 4645.

[7] C. Liu, B. C. Colón, M. Ziesack, P. A. Silver, D. G. Nocera, *Science* **2016**, *352*, 1210.

[8] M. G. Walter, E. L. Warren, J. R. McKone, S. W. Boettcher, Q. Mi, E. A. Santori, N. S. Lewis, *Chem. Rev.* **2010**, *110*, 6446.

[9] I. Staffell, D. Scamman, A. Velazquez Abad, P. Balcombe, P. E. Dodds, P. Ekins, N. Shah, K. R. Ward, *Energy Environ. Sci.* **2019**, *12*, 463.

[10] Y. Goto, T. Hisatomi, Q. Wang, T. Higashi, K. Ishikiriyama, T. Maeda, Y. Sakata, S. Okunaka, H. Tokudome, M. Katayama, S. Akiyama, H. Nishiyama, Y. Inoue, T. Takewaki, T. Setoyama, T. Minegishi, T. Takata, T. Yamada, K. Domen, *Joule* **2018**, *2*, 509.

[11] Y. Ma, X. Wang, Y. Jia, X. Chen, H. Han, C. Li, *Chem. Rev.* **2014**, *114*, 9987.

[12] X. Chen, L. Liu, F. Huang, *Chem. Soc. Rev.* **2015**, *44*, 1861.

[13] A. B. Murphy, P. R. F. Barnes, L. K. Randeniya, I. C. Plumb, I. E. Grey, M. D. Horne, J. A. Glasscock, *Int. J. Hydrogen Energy* **2006**, *31*, 1999.

[14] J. H. Kim, D. Hansora, P. Sharma, J.-W. Jang, J. S. Lee, *Chem. Soc. Rev.* **2019**, *48*, 1908.

[15] Q. Liu, J. He, T. Yao, Z. Sun, W. Cheng, S. He, Y. Xie, Y. Peng, H. Cheng, Y. Sun, Y. Jiang, F. Hu, Z. Xie, W. Yan, Z. Pan, Z. Wu, S. Wei, *Nat. Commun.* **2014**, *5*, 5122.

[16] L. Yu, H. Hu, H. B. Wu, X. W. Lou, *Adv. Mater.* **2017**, *29*, 1604563.

[17] P. Zhang, X. W. Lou, *Adv. Mater.* **2019**, *31*, 1900281.

[18] S. Wang, B. Y. Guan, Y. Lu, X. W. Lou, *J. Am. Chem. Soc.* **2017**, *139*, 17305.

[19] P. Zhang, S. Wang, B. Y. Guan, X. W. Lou, *Energy Environ. Sci.* **2019**, *12*, 164.

[20] Y. Fu, D. Sun, Y. Chen, R. Huang, Z. Ding, X. Fu, Z. Li, *Angew. Chem. Int. Ed.* **2012**, *51*, 3364.

[21] Z. Wang, X. Li, H. Xu, Y. Yang, Y. Cui, H. Pan, Z. Wang, B. Chen, G. Qian, *J. Mater. Chem. A* **2014**, *2*, 12571.

[22] P. Wang, J. Lang, D. Liu, X. Yan, *Chem. Commun.* **2015**, *51*, 11370.

[23] E. S. Kim, N. Nishimura, G. Magesh, J. Y. Kim, J.-W. Jang, H. Jun, J. Kubota, K. Domen, J. S. Lee, *J. Am. Chem. Soc.* **2013**, *135*, 5375.

[24] H. Zhang, S. O. Park, S. H. Joo, J. H. Kim, S. K. Kwak, J. S. Lee, *Nano Energy* **2019**, *62*, 20.

[25] A. Kafizas, X. Wang, S. R. Pendlebury, P. Barnes, M. Ling, C. Sotelo-Vazquez, R. Quesada-Cabrera, C. Li, I. P. Parkin, J. R. Durrant, *J. Phys. Chem. A* **2016**, *120*, 715.

[26] Y. Gao, J. Zhu, H. An, P. Yan, B. Huang, R. Chen, F. Fan, C. Li, *J. Phys. Chem. Lett.* **2017**, *8*, 1419.

[27] H. Zhang, J. H. Kim, J. H. Kim, J. S. Lee, *Adv. Funct. Mater.* **2017**, *27*, 1702428.

[28] E. Courtin, G. Baldinozzi, M. T. Sougrati, L. Stievano, C. Sanchez, C. Laberty-Robert, *J. Mater. Chem. A* **2014**, *2*, 6567.

[29] Z. Lou, Y. Li, H. Song, Z. Ye, L. Zhu, *RSC Adv.* **2016**, *6*, 45343.

Figures and Captions

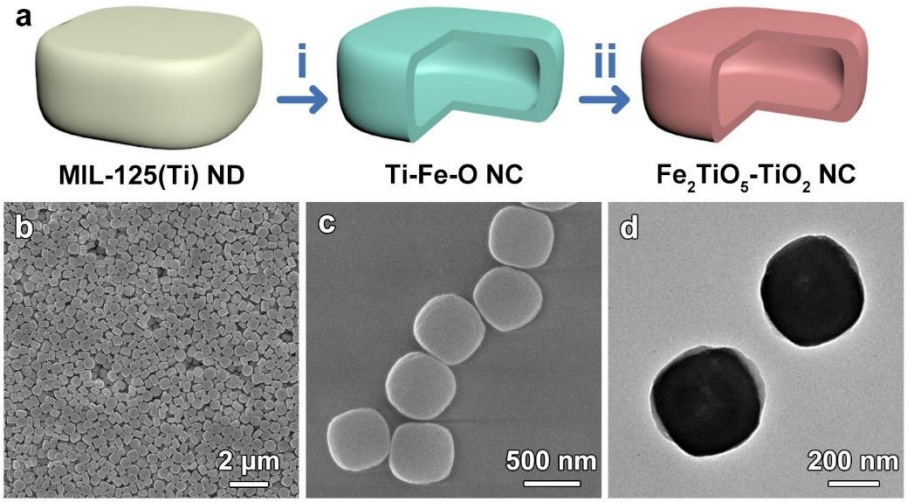

Figure 1. (a) Schematic illustration of the synthetic procedures of Fe_2TiO_5-TiO_2 NCs: (i) hydrothermal reaction and (ii) annealing. (b, c) FESEM and (d) TEM images of MIL-125(Ti) NDs.

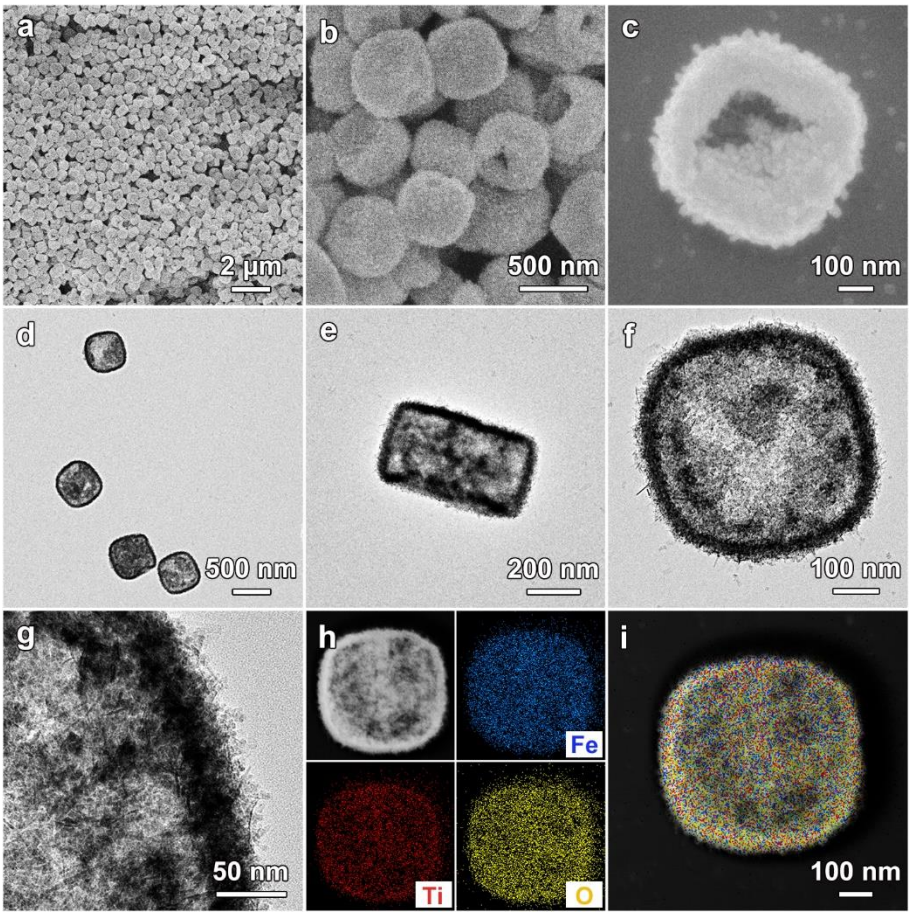

Figure 2. (a-c) FESEM and (d-g) TEM images of Ti-Fe-O NCs. (h) HAADF-STEM image of a Ti-Fe-O NC with elemental mapping images for Fe, Ti, and O. (i) Overlay image of the corresponding mapping images in (h).

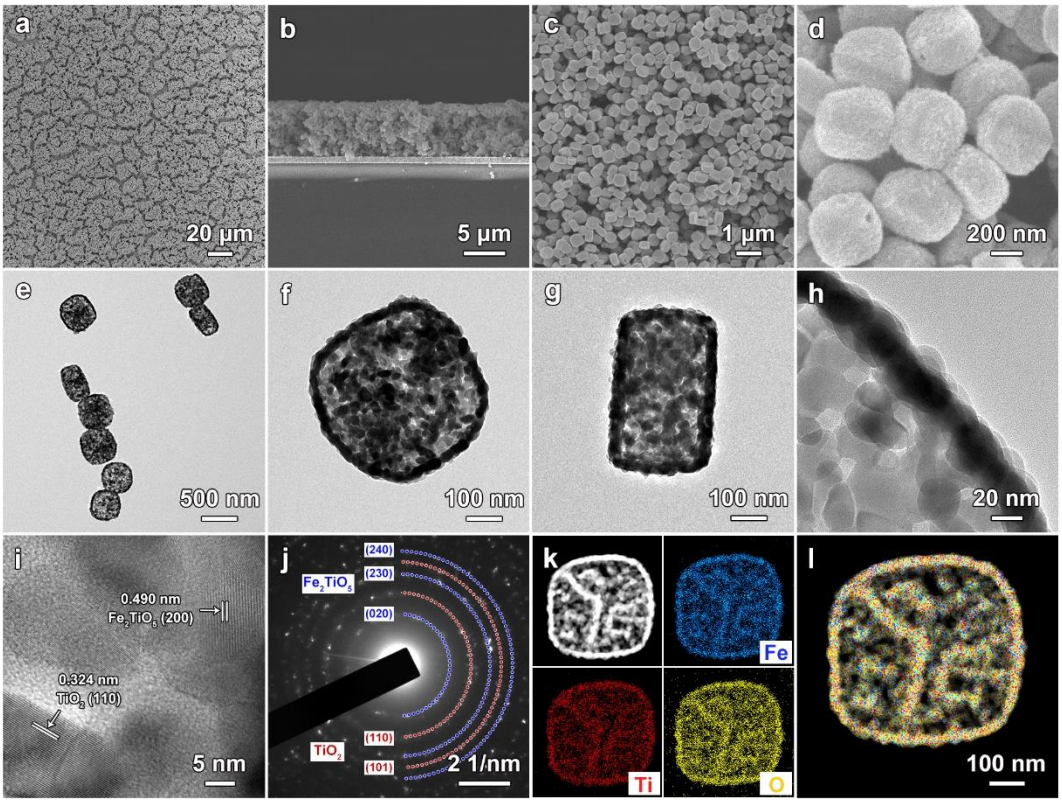

Figure 3. (a) Top-view and (b) side-view FESEM images of the Fe_2TiO_5-TiO_2 NC photoanode. (c, d) FESEM, (e-h) TEM, (i) HRTEM images and (j) SAED pattern of Fe_2TiO_5-TiO_2 NCs. (k) HAADF-STEM image of a Fe_2TiO_5-TiO_2 NC with elemental mapping images for Fe, Ti and O. (l) Overlay image of the corresponding mapping images in (k).

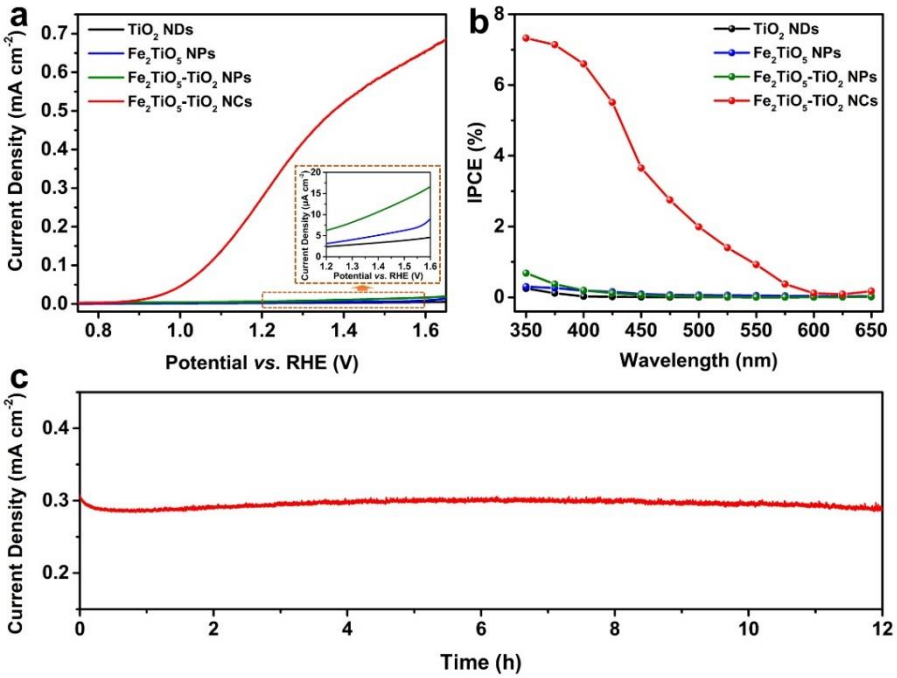

Figure 4. (a) *J*-*V* curves and (b) IPCEs of TiO_2 NDs, Fe_2TiO_5 NPs, Fe_2TiO_5-TiO_2 NPs and Fe_2TiO_5-TiO_2 NCs. (c) *J*-t curve of Fe_2TiO_5-TiO_2 NCs. The inset in (a) shows the enlarged view of several curves.

for Table of Content Entry

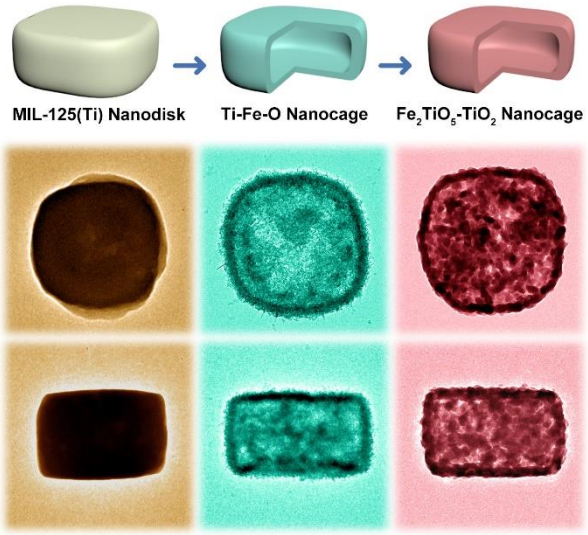

Heterostructured Fe_2TiO_5-TiO_2 nanocages are fabricated through a facile synthetic approach. With the advantages of the novel hollow heterostructure, the well-defined $FeTi_2O_5$-TiO_2 nanocages exhibit enhanced photoelectrochemical performance compared with TiO_2 nanodisks, Fe_2TiO_5 nanoparticles, and Fe_2TiO_5-TiO_2 nanoparticles.